HHS Public Access

Author manuscript

ACS Infect Dis. Author manuscript; available in PMC 2021 May 24.

Published in final edited form as:

ACS Infect Dis. 2020 February 14; 6(2): 302–312. doi:10.1021/acsinfecdis.9b00382.

Tight-binding Hydroxypyrazole HIV-1 Nef Inhibitors Suppress Viral Replication in Donor Mononuclear Cells and Reverse Nef-mediated MHC-I downregulation

Haibin Shi[1], **Colin M. Tice**[2], **Lori Emert-Sedlak**[1], **Li Chen**[1], **Wing Fai Li**[1,#], **Marianne Carlsen**[2], **Jay E. Wrobel**[2], **Allen B. Reitz**[2], **Thomas E. Smithgall**[1,*]

[1]Department of Microbiology and Molecular Genetics, University of Pittsburgh School of Medicine, Suite 523 Bridgeside Point II, 450 Technology Drive, Pittsburgh Pennsylvania, 15219, United States

[2]Fox Chase Chemical Diversity Center, Inc., Pennsylvania Biotechnology Center, 3805 Old Easton Road, Doylestown, Pennsylvania, 18902, United States

Abstract

The HIV-1 Nef accessory factor is critical to the viral life cycle *in vivo* and promotes immune escape of infected cells via downregulation of cell-surface MHC-I. Previously we discovered small molecules that bind directly to Nef and block many of its functions, including enhancement of viral infectivity and replication in T cell lines. These compounds also restore cell-surface MHC-I expression in HIV-infected CD4 T cells from AIDS patients, enabling recognition and killing by autologous CTLs. In this study, we describe the synthesis and evaluation of a diverse set of analogs based on the original hydroxypyrazole Nef inhibitor core. All analogs were screened for interaction with recombinant HIV-1 Nef by surface plasmon resonance (SPR) and for antiretroviral activity in TZM-bl reporter cells infected with HIV-1. Active analogs were ranked based on an activity score that integrates three aspects of the SPR data (affinity, residence time, and extent of binding) with antiretroviral activity. The top scoring compounds bound tightly to Nef by SPR, with K_D values in the low nM to pM range, and displayed very slow dissociation from their Nef target. These analogs also suppressed HIV-1 replication in donor PBMCs with IC_{50} values in the 1–10 nM range without cytotoxicity, inhibited Nef-mediated Itk and Hck tyrosine kinase activation, and rescued MHC-I downregulation in a Nef-transfected T cell line. Development of Nef inhibitors based on the structure-activity relationships defined here have promise as a new approach to antiretroviral therapy that includes a path to eradication of HIV-infected cells via the adaptive immune response.

Graphical Abstract

[*]Correspondence: Thomas E. Smithgall, Ph.D. Department of Microbiology and Molecular Genetics, University of Pittsburgh School of Medicine, Bridgeside Point II, Suite 523, 450 Technology Drive, Pittsburgh, PA 15219, Tel. 412-648-8106, Fax 412-624-8997, tsmithga@pitt.edu.

[#]Present address: Tsinghua University School of Medicine, Beijing 100084, China

ASSOCIATED CONTENT

Supporting information

Figures S1 - S4, Tables S1 - S3, and details of materials and methods including medicinal chemistry data.

The authors declare no competing financial interests.

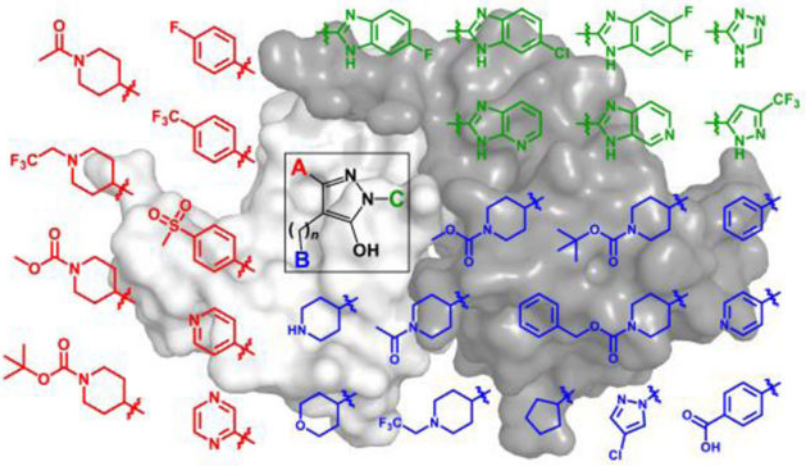

Keywords

HIV/AIDS; antiretroviral drug development; HIV-1 Nef inhibitors; HIV accessory proteins; surface plasmon resonance

While combination antiretroviral therapy has transformed HIV-1 infection from a life-threatening illness to a chronic condition, these drugs do not clear the virus from the patient and life-long administration is required to prevent relapse. Chronic antiretroviral drug exposure over decades causes metabolic disturbances, organ damage, and promotes drug resistance.[1] These issues underscore the urgent need for new pharmaceutical agents to combat HIV disease, with a focus on functional cure through the elimination of latent viral reservoirs.[2]

Current antiretroviral drugs block the activity of HIV-1 enzymes critical to the viral life cycle, including reverse transcriptase, integrase and protease, as well as viral entry.[3] The HIV-1 genome also encodes four unique accessory factors (Vpr, Vpu, Vif, and Nef) essential for viral pathogenicity that represent alternative targets for drug discovery.[4–6] Nef is particularly attractive in this regard, because of its essential role in HIV-1 pathogenesis and AIDS progression.[7–11] Nef is a relatively small protein (27–30 kDa, depending on the viral isolate) that is packaged in the virion and is also expressed at high levels early in the viral life cycle. Nef interacts with a diverse group of host cell proteins, providing the mechanistic basis for its functions. These include downregulation of cell-surface immune (MHC-I/II) and viral (CD4/CXCR4/ CCR5) receptors,[12,13] counteracting host cell restriction factors (e.g. SERINC5 and Ezrin),[14–16] remodeling of the actin cytoskeleton,[17] and stimulation of host cell signaling pathways (e.g. Tec[18,19] and Src[20] family kinases) to favor viral replication. Through these mechanisms, Nef allows HIV-infected cells to avoid immune surveillance by the host, prevents viral superinfection, and enhances viral infectivity and spread.

Nef has a critical role in many aspects of the HIV-1 life cycle, making it a rational antiretroviral drug target. However, Nef lacks intrinsic enzymatic or biochemical activity, and functions instead via interactions with diverse host proteins that regulate cell signaling, protein trafficking, and the cytoskeleton as described above. X-ray crystallography of

Nef•effector complexes shows that distinct surfaces of the Nef protein are involved in these protein-protein interactions, complicating rational design of a universal Nef inhibitor capable of blocking its pleiotropic actions[21–23]. In previous work, we addressed this issue by developing a high-throughput screening (HTS) assay for inhibitors of Nef-dependent activation of a protein kinase partner, the Src-family kinase Hck[24]. HTS of more than 220,000 compounds using this kinase-coupled screening approach identified a unique inhibitor based on a hydroxypyrazole scaffold. This compound, a diphenyl hydroxypyrazolodiazene known as **B9**, demonstrated inhibitory activity against multiple Nef functions including enhancement of viral infectivity, replication, as well as MHC-I downregulation[24,25]. In the present study, we used this compound as a starting point for the synthesis of a diverse collection of more than 200 analogs and assessed their efficacy using surface plasmon resonance (SPR) to evaluate the kinetics, affinity and extent of binding to Nef in vitro along with a cell-based assay for antiretroviral activity. Binding and antiretroviral activity data for each compound were then integrated as a single activity score, which permitted ranking of the active analogs. The top-scoring compounds from this approach were found to potently inhibit Nef-mediated enhancement of HIV-1 replication in donor PBMCs, while retaining the ability to reverse MHC-I downregulation in Nef-transfected cells. These active compounds share structural features that define a Nef inhibitor pharmacophore for the first time, and provide a path to a new class of antiretroviral drugs with the potential to reduce or eliminate latent viral reservoirs by enabling the host immune response.

RESULTS AND DISCUSSION

Characterization of inhibitor analog binding to recombinant Nef by surface plasmon resonance (SPR).

Using the hydroxypyrazole core of **B9** as a starting point, we synthesized a library of 216 diverse analogs with unique functionalities. Figure 1 shows representative examples of substitutions that replaced the A, B, and C positions of this original hit compound. Our structure-activity approach led to the identification of new analogs with enhanced affinity for Nef and potent antiretroviral activity while maintaining the ability to reverse Nef-mediated downregulation of MHC-I from the cell surface.

All inhibitor analogs were screened for direct interaction with purified Nef in vitro using an SPR assay. This approach allows for assessment of analog interaction with Nef in real time, and subsequent evaluation of binding kinetics as well as the lifetime of the Nef•inhibitor complex. For these experiments, recombinant full-length HIV-1 Nef protein (from HIV-1 strain NL4–3) was expressed in bacteria and purified to homogeneity. The Nef protein was then immobilized on the SPR biosensor surface, and each compound was injected over a range of concentrations. Association and dissociation kinetics were then best-fit using either a 1:1 Langmuir binding model or a two-step induced-fit model, and the resulting kinetic constants were used to generate K_D values. In addition, the stability of each Nef•inhibitor complex was defined by its residence time (T), which is calculated from the reciprocal of the dissociation rate constant ($1/k_{off}$). Residence time may provide a better indication of drug

action in vivo than K_D, because it reflects the period of time that the drug interacts with its target even after plasma levels begin to recede[26].

Evaluation of the SPR data for all inhibitors revealed distinct interaction behaviors with respect to affinity (K_D value), residence time, as well as extent of interaction (measured in response units or RU), with representative examples shown in Figure 2. Some analogs bound with relatively high affinities, with K_D values in the low nM to pM range, and also showed relatively strong SPR responses, with RU values in the 20 to 40 range at an analog concentration of 30 μM (RU_{30}; exemplified by compound **FC-7098** in Figure 2). Inhibitors of this type also dissociated relatively rapidly from Nef, with the sensorgrams best-fit by a simple 1:1 Langmuir model. Other analogs also demonstrated high affinity with short residence times, but showed a lower overall SPR response (with RU_{30} values < 10; e.g. compound **FC-8107**). Some analogs bound with high affinity and displayed very slow dissociation, resulting in long residence times (e.g., **FC-8517**). Sensorgrams of this type were often best-fit by a two-step, induced-fit model, which is consistent with a ligand-induced conformational change in Nef. Finally, 53 of the 216 analogs tested showed no detectable interaction with Nef by SPR (e.g. **FC-8972**). These non-binding compounds provide important clues to the structure-activity relationship for this class of Nef inhibitors, as described in more detail below. SPR data for all analogs that bound to Nef, including the kinetic K_D values, residence time and extent of binding, are summarized in the Supporting Information (Table S1) along with the chemical structure for each compound.

Assessment of antiretroviral activity.

Antiretroviral activity of the hydroxypyrazole Nef inhibitor analogs was assessed using the reporter cell line, TZM-bl. These cells are engineered to express the receptors for HIV-1 (CD4 and CXCR4) and also harbor an integrated copy of the HIV-1 LTR linked to firefly luciferase[27]. Infection of TZM-bl cells with HIV-1 induces Tat-dependent transcription from the integrated LTR, leading to a strong luciferase signal. The infectivity of HIV-1 in this system is enhanced by 3- to 5-fold in the presence of Nef, providing a convenient assay to screen analogs for Nef-dependent antiretroviral activity[24].

All 216 analogs were screened in TZM-bl cells at a final concentration of 1 μM, and percent infectivity inhibition was then plotted against the kinetic K_D value obtained by SPR (Supporting Information, Figure S1A). Forty-two analogs with K_D values of 100 nM or less inhibited HIV-1 infectivity by at least 10% at 1 μM, while 11 of these inhibited infectivity by 90% or more. On the other hand, 10 of the 42 analogs with K_D values ≤ 100 nM inhibited viral infectivity by less than 10% at this concentration, which may reflect poor cellular uptake or non-productive interaction with the Nef protein. Among the 216 analogs tested, 2 analogs that bound Nef weakly (K_D values > 10 μM) blocked HIV-1 replication by more than 90%. Although these 2 analogs represent a very small proportion of the total, this observation illustrates the possibility of off-target effects that could also affect HIV-1 replication in the TZM-bl cell system.

For comparison, we also plotted the antiviral activity of each analog as a function of residence time on the Nef protein target (Figures S1B and S1C). In this case, 47 analogs with residence times greater than 60 minutes inhibited HIV-1 infectivity by at least 10% at 1

μM, while 11 of these displayed potent antiretroviral activity (> 90% inhibition of infectivity). As in the prior analysis based on K_D values, 10 compounds in this group of 47 showed less than 10% inhibition of infectivity, indicative of poor cell penetration or non-productive target interaction. Out of the 216 analogs tested, just 9 compounds with relatively short residence times (T < 60 min) blocked replication by more than 90%. The poor correlation between residence time and antiviral activity may indicate off-target effects in these limited cases.

We then compared the sets of analogs with K_D values ≤ 100 nM or target residence time greater than 60 minutes that showed at least 10% inhibition of HIV-1 infectivity at 1.0 μM in each case. Forty analogs were common to both analyses, with 2 compounds unique to the affinity-based analysis and 7 unique to scoring based on residence time (Figure S1D). While the overlap between the two groups is substantial, it is not complete. Furthermore, this approach does not provide a clear ranking of active inhibitors for follow-up studies. This led us to develop an integrated approach to identify the most active analogs for further development as described in the next section.

Integration of SPR data and antiretroviral activity enables ranking of Nef inhibitor analog efficacy.

Simple two-dimensional data analysis described in the previous section shows that assessment of Nef inhibitor efficacy based on antiretroviral activity as a function of either K_D value or on-target residence time yields only partial overlap in terms of active compounds. This approach also is based on arbitrary standards for both the SPR data and the antiretroviral effects, and does not quantitatively identify the most active compounds for follow-up. Furthermore, neither analysis considers the extent of analog binding to the Nef protein by SPR, which is directly proportional to the RU_{max} at equilibrium. To integrate multiple SPR parameters with antiretroviral activity in a single numerical value, we devised an ‘Activity Score’ for each analog that enabled an unbiased ranking. The Activity Score was first defined as the product of the residence time (Log_{10} T, where $T = 1/k_{off}$), the SPR response at the maximum concentration tested as an approximation of the RU_{max} (30 μM; normalized to the amount of Nef protein bound to the biosensor, also in RU) and the percent inhibition of infectivity in the TZM-bl reporter cell assay. A z-score statistic was then generated for each analog from the mean of all non-zero Activity Scores according to the formula, $z = (AS_x\text{-}AS_m)/SD$, where AS_x is the Activity Score for a given compound, AS_m is the mean score for all active compounds (n = 170), and SD is the standard deviation from the mean. Figure 3A shows the z-score ranking for all active compounds based on residence time. This approach identified 8 analogs with z-scores > 2.0 (i.e., with values greater than two standard deviations above the mean). We then repeated this analysis, using the K_D value for each analog (as $-Log_{10}$ K_D) in place of the residence time, with the other two factors remaining the same. Figure 3B shows the activity score ranking resulting from the K_D-based approach, which identified 9 analogs with z-scores > 2.0. A comparison of the top compounds from both rankings identified 6 analogs in common, which are discussed in the next section. Biochemical and biological data for these analogs are summarized in Table S2.

Top-scoring Nef inhibitors share structural features.

Parallel Activity Score analysis based on affinity or residence time identified six compounds common to both rankings: **FC-7902**, **FC-7943**, **FC-7976**, **FC-8052**, **FC-8517**, and **FC-8698**. Figure 4 shows the structures of these compounds along with their SPR sensorgrams, all of which were best-fit by the two-step induced-fit model. In this binding model, the first step involves 1:1 interaction between the ligand and the Nef protein, to form a lower affinity complex. This initial complex can either dissociate, or undergo a conformational change to a higher affinity complex. The fitting software uses the kinetic constants that govern transitions between both states to calculate an overall kinetic K_D value. The top six analogs bound Nef with K_D values ranging from about 60 pM (**FC-7943**) to 10 nM (**FC-8698**). While these K_D values provide a useful parameter for comparative analysis of direct analog interaction with Nef in vitro, they are not necessarily predictive of inhibitor potency or efficacy in HIV-infected cells. In the cellular context, Nef is associated with lipid bilayers where it interacts with multiple host cell proteins, including kinases, receptors, and endocytic trafficking adaptors (see Introduction). Although the recombinant Nef protein population is immobilized on a two-dimensional polydextran hydrogel surface during the SPR assay, the influence of the lipid bilayer and partner protein interaction are not represented. Both of these factors are very likely to influence Nef structure and dynamics as well as inhibitor action in the cellular environment.

The remarkably low K_D values observed with several of the top six Nef inhibitor analogs reflect their very slow dissociation kinetics from the Nef protein (long residence times). Inspection of the SPR sensorgrams shows that none of these analogs completely dissociated from their protein target over the relatively short dissociation phase of each SPR experiment (3 minutes), suggesting that these inhibitors may induce a conformation of Nef to which they bind tightly. This is particularly striking for analogs **FC-8052** and **FC-8698**, which show very little reduction in the SPR signal during the dissociation phase (Figure 4). Note that all six compounds dissociated completely during regeneration of the Nef biosensor under reducing conditions with a shift in pH (not shown). This observation suggests that while these analogs are tightly bound to Nef, the interaction is not covalent.

Inspection of the structures of the top six analogs reveals some shared features (Figure 4). All six analogs share the common hydroxypyrazole core joined to either a benzimidazole (**FC-7902**, **FC-7696**, **FC-8517**), aza-benzimidazole (**FC-7943**), or chloro-benzimidazole group (**FC-8052**, **FC-8698**) at the C-position. At the A-position of the hydroxypyrazole core, three analogs (**FC-7902**, **FC-7943**, **FC-7976**) share a phenyl group substituted at the *para* position by a hydrophobic trifluoromethyl group, although other less hydrophobic groups are accommodated at this position including *para*-(methylsulfonyl)phenyl (**FC-8517**) and a *tert*-butyl piperidine carboxylate (**FC-8052**), as well as the unsubstituted phenyl (**FC-8698**). At the B-position of the hydroxypyrazole, three analogs share a fluorophenethyl side chain (**FC-7943**, **FC-8052**, **FC-8517**). The remaining analogs exhibit methoxycarbonylphenethyl (**FC-8698**), pyridylethyl (**FC-7976**), or cyclopentylmethyl (**FC-7902**) groups at this position.

Inspection of analog structures unique to the activity score analysis based on residence time (z-score > 2.0) provides some additional insight regarding the structure activity relationship (Supporting Information, Figure S2). This group includes two compounds, **FC-7868** and **FC-8007**, both of which are very similar in structure to **FC-7943** with differences limited to the benzimidazole moiety. These compounds both show high RU values and very slow dissociation from Nef. Analogs unique to the activity score ranking based on K_D values also show structural similarity with the top six compounds. Analog **FC-8700** shares chlorobenzimidazole and fluorophenethyl substituents with several top analogs, with a fluorophenyl group at the A-position of the hydroxypyrazole, while **FC-8676** replaces the trifluoromethylphenyl group in **FC-7868** with a cyclopropane moiety. Finally, **FC-7946** is identical to **FC-7943**, **FC-7898**, and **FC-8007** at the A and B positions of the hydroxypyrazole, but the benzimidazole is replaced with a trifluoromethylpyrazole group. These results demonstrate the remarkably diverse nature of the substituent combinations that can be added to the hydroxypyrazole core while retaining potency and efficacy in terms of direct binding to their Nef target and antiretroviral activity in the TZM-bl assay. This observation likely reflects the dynamic nature of the Nef protein, which recruits multiple classes of host cell effectors by adopting unique conformations[21–23,28]. The same may be true for hydroxypyrazole Nef inhibitors, with unique modifications in each compound able to induce local changes in the conformation of the Nef protein to optimize interaction.

Inspection of analog structures that showed little or no binding to Nef by SPR also inform the structure-activity relationship. Replacement of the hydroxyl group in the hydroxypyrazole core present in all active compounds with a primary amine (**FC-9120**) or hydrogen (**FC-10690**) completely abolishes binding as well as antiretroviral activity (Supporting Information, Figure S3A). This is also true when the hydroxypyrazole oxidizes to the hydroxycarbonyl (**FC-8006**). Furthermore, substitutions at the A and B positions of the pyrazole are both essential for interaction in the SPR assay. Examples include **FC-7697**, which lacks the trifluoromethylphenyl group found in active analog **FC-7976**, as well as **FC-7700**, which lacks the fluorophenethyl common to multiple active analogs (Figure S3B). Other analogs lacking the 4-fluorophenethyl or other groups at position B showed lower affinity, very short residence times, and exhibited no antiretroviral activity (e.g. **FC-7698**, **FC-7719**, and **FC-7793**; Table S1). Analogs with extended ring structures in the A-position of the hydroxypyrazole also showed diminished binding, such as **FC-7996**, **FC-8000**, and **FC-8057**, suggesting that these larger moieties may access a pocket of limited size within the Nef structure (Figure S3C). Removal of the benzimidazole group from several of the most active compounds (**FC-8700**, **FC-8698**, **FC-8052**, **FC-7943**) substantially reduced binding and antiretroviral activity in the infectivity assay, demonstrating the importance of this group to the overall SAR (Figure S4).

Top-scoring Nef inhibitors potently suppress Nef-dependent enhancement of HIV-1 replication in primary host cells.

Previous studies with first-generation Nef inhibitors based on the hydroxypyrazole scaffold showed that they inhibit Nef-dependent enhancement of HIV-1 replication in T cell lines.[24] To extend these studies to a more relevant system for HIV-1, we used peripheral blood mononuclear cells (PBMCs) from HIV-negative donors. PBMCs were isolated from buffy

coats, stimulated in vitro with PHA and IL-2, and then infected with either wild-type HIV-1 or a mutant that fails to express Nef (ΔNef). Viral replication was assessed 4 days later as the titer of p24 capsid protein present in the culture supernatant. Figure 5A shows a comparison of wild-type vs. ΔNef HIV-1 replication over a range of viral inocula from a representative donor. This result shows that Nef enhances HIV-1 replication at low to moderate viral inputs, but that the effect is overcome at higher levels of infection as observed previously in T cell lines[24,29]. Enhancement of HIV-1 replication by Nef was consistently observed across multiple donors, despite variation in the overall extent of replication (Figure 5B). All donors were tested in this manner to demonstrates Nef-dependent enhancement of HIV-1 replication prior to analog testing.

We next explored the antiretroviral activity of the top-scoring Nef inhibitor analogs in HIV-infected PBMCs under conditions where replication was enhanced by Nef. Each compound was added over a 3-log range of concentrations (1 to 1,000 nM), and viral replication assayed by p24 Gag AlphaLISA as before. Cell viability was assessed in parallel in uninfected PBMCs over the same range of inhibitor concentrations. IC_{50} values for inhibition of viral replication, CC_{50} values for cytotoxicity, and the resulting therapeutic indices are summarized in Table 1. Five of the six top compounds inhibited Nef-dependent enhancement of HIV-1 replication in PBMCs in the low nM range. The most potent inhibitor was **FC-8052**, with an IC_{50} value of 0.65 nM. With all six compounds, inhibition of viral replication occurred without appreciable toxicity. CC_{50} values ranged from 0.7 to 1 μM, yielding therapeutic indices of two orders of magnitude or more for the inhibitors with IC_{50} values in the single-digit nM range (Table 1).

Nef inhibitor analogs block Nef-dependent kinase activation.

Previous studies have shown that the IL-2-inducible tyrosine kinase, Itk, is critical to several stages of the HIV-1 life cycle in CD4 T cells.[30] Itk is a member of the Tec/Btk family of non-receptor tyrosine kinases, and normally participates in T cell receptor signal transduction.[31] HIV-1 Nef has been shown to associate directly with Itk and induce its activation, providing a mechanism to short-circuit TCR activation for the benefit of the virus.[18] Selective inhibitors of Itk kinase activity, as well as siRNA Itk knockdown, both inhibit HIV-1 replication in T cell lines and primary CD4 T cells.[18,30] Together, these observations suggest that hydroxypyrazole Nef inhibitors described here may interfere with Nef-mediated activation of Itk as one mechanism by which they suppress HIV-1 replication in PBMCs. To test this idea, we adapted a cell-based bimolecular fluorescence complementation (BiFC) assay previously developed by our group[18] to determine the effect of compound treatment on Itk activation by Nef as well as the interaction of the two proteins. Nef and Itk were fused to non-fluorescent, complementary fragments of the GFP variant, Venus.[32] Itk was fused to the C-terminal fragment of Venus (Itk-VC), and expressed either alone or in the presence of the complementary Nef-VN fusion protein in 293T cells. The cells were then immunostained with antiphosphotyrosine (pTyr) and Itk antibodies and imaged by three-color confocal microscopy for kinase activity (pTyr signal), Itk expression, and Itk interaction with Nef (BiFC signal; Figure 6A). When expressed alone, Itk shows weak pTyr fluorescence. However, when co-expressed with Nef, the two proteins interact at the plasma membrane (BiFC signal) and exhibit a stronger pTyr signal, indicative of Itk

activation by Nef. As a control, we also included a Nef mutant that is defective for homodimerization, in which Leu112 and Tyr115 are replaced with aspartate (Nef-DD). These two residues map to the Nef dimerization interface in several X-ray crystal structures,[23,33] and are required for Nef homodimerization in cell-based BiFC assays.[34] The Nef-DD mutant interacts with Itk (positive BiFC signal) but is unable to stimulate Itk kinase activity (pTyr signal equivalent to Itk alone), demonstrating an essential role for Nef homodimer formation in the Itk activation mechanism. To quantitate the results, single-cell mean fluorescence intensities for the pTyr and Itk protein expression signals from a minimum of 100 cells were determined using ImageJ, and are plotted as pTyr:Itk protein ratios in Figure 6B. Expression of Nef induced a significant increase in Itk activity ($p < 0.0001$), while the Nef-DD mutant did not, confirming the role of the Nef homodimer in Itk activation.

Using this system, we tested the effect of **B9** and the top six Nef inhibitor analogs from the activity score ranking on Nef-dependent activation of Itk. **B9** and five of the six analogs completely suppressed Itk activation by Nef ($p < 0.0001$); **FC-7976** treatment also reduced activity but was not statistically significant. Importantly, addition of the compounds to cells expressing Itk alone had no effect on basal kinase activity, demonstrating that they affect Itk activation via Nef and not through direct inhibition of the kinase (data not shown). Since Itk activation requires the Nef homodimer, the active compounds may work by disrupting the Nef dimer or leading to an alternative dimer conformation incompatible with kinase activation.

In addition to Itk, Nef also interacts with and activates members of the Src kinase family expressed in macrophages (Hck) and in T cells (Lyn).[35] Previous work has shown that inhibition of Nef-mediated Src-family kinase activation with **B9** or directly with ATP-site kinase inhibitors suppresses HIV-1 infectivity and replication.[24,36] To determine whether hydroxypyrazole Nef inhibitor analogs also influence Src-family kinase activation by Nef, we established an analogous 293T cell BiFC assay using Nef and Hck. As with Itk, wild-type Nef significantly enhanced Hck activation at the membrane in this system, while the dimerization-defective Nef-DD mutant failed to do so despite retaining interaction with Hck (Figure 6A and 6C). **B9** and five of the six top analogs completely suppressed Nef-dependent Hck activation ($p < 0.0001$), with the exception of analog **FC-7976**. Together with the Itk data, these results suggest that hydroxypyrazole Nef inhibitors attenuate HIV-1 replication in PBMCs by interfering with kinase signaling pathways through a mechanism that may involve disruption of the Nef homodimer. This observation is consistent with the results from the original screening assay used to discover **B9**, which was based on the inhibition of Nef-induced activation of recombinant Hck *in vitro*.[24]

Assessment of Nef inhibitor analogs on MHC-I downregulation.

Nef is well-known to prevent cell-surface display of MHC-I in complex with HIV-1 antigenic peptides on infected cells, promoting escape from detection by cytotoxic T lymphocytes.[12,37] As a consequence, this effect of Nef prevents clearance of the virus from the infected host, and may contribute to establishment and maintenance of the persistent viral reservoir. In previous studies, we established that the original hydroxypyrazole Nef inhibitor identified by HTS (**B9**), as well as first-generation **B9** analogs, restored MHC-I to

the surface of HIV-infected CD4+ T cells.[25] Moreover, when inhibitor-treated cells were co-cultured with autologous CD8 T cells expanded in the presence of HIV-1 antigenic peptides, the CD8 T cells were activated and displayed CTL responses against the infected target cells. This result suggests that Nef inhibitors have the potential to enhance CTL-mediated responses against HIV+ cells in vivo as part of a strategy to clear the latent viral reservoir.

Based on these previous results, we screened top-scoring Nef inhibitor analogs for their ability to rescue Nef-mediated MHC-I downregulation using CEM-SS cells as a model system. This T cell line is engineered to express the MHC class I allele HLA-A*02, and transfection of these cells with a Nef expression vector results in robust downregulation[38]. Use of this Nef-transfected cell line separates the effect of Nef on MHC-I from effects on viral infectivity and replication, thus simplifying interpretation of the results. The vector also carries a second expression cassette for GFP, which allows for gating of the transfected cell population by flow cytometry. CEM-SS cells transfected with the Nef expression vector or GFP alone were fixed and stained with antibodies to HLA-A*02, and analyzed by two-color flow cytometry to detect the level of cell-surface MHC-I in the GFP-positive cell population. GFP+/Nef+ cells demonstrated a consistent decrease in cell-surface MHC-I staining compared to control cells expressing GFP alone (representative example shown in Figure 7A). Cells transfected with the dimerization-defective Nef mutant (Nef-DD) showed attenuated MHC-I downregulation, providing an additional negative control. We then tested top-scoring Nef inhibitor analogs for rescue of cell-surface MHC-I in Nef-expressing cells, including the six analogs from Figure 4 plus **FC-8007** and **FC-8700** (see Figure S2 for structures). All eight analogs tested rescued Nef-dependent MHC-I downregulation, with seven compounds displaying rescue activity greater than that of **B9**. Note that while the effect of the parent compound (**B9**) on rescue of Nef-mediated MHC-I downregulation in the CEM-SS cell system is relatively modest (about 4% at 1.0 μM), this compound restored sufficient MHC-I to the surface of AIDS patient-derived CD4 cells to trigger CD8 CTL responses.[25] Thus, the extent of MHC-I rescue observed with new analogs in Nef-transfected CEM-SS cells is predicted to translate into induction of CTL responses against HIV-infected CD4 T cells in the context of viral infection. Overall, these results are important because they establish that chemical modifications can be made to the original inhibitor structure without compromising antagonism of Nef-mediated MHC-I downregulation. This unique feature of Nef inhibitors may help reduce the size of HIV-1 reservoirs in addition to suppressing viral replication.

Liver microsomal stability assays of Nef inhibitor analogs.

As a first step towards assessment of Nef inhibitor efficacy in vivo, we tested the sensitivity of the top-scoring inhibitors as well as several other representative compounds to metabolism by mouse liver microsomes in vitro (Table S3). Analogs **FC-7943** and **FC-8517** showed excellent microsomal stability, with half-lives of 154 and > 180 minutes, respectively. Analogs **FC-7902**, **FC-7946**, **FC-7976**, and **FC-8698** showed intermediate stability, with half-lives ranging from 35 to 52 minutes, while compounds **FC-7868** and **FC-8052** were rapidly metabolized, with half-lives of 23 and 12 minutes.

SUMMARY AND CONCLUSIONS

This report describes synthesis and evaluation of a diverse group of potent hydroxypyrazole antagonists of multiple HIV-1 Nef functions, including enhancement of viral infectivity and replication, host cell kinase activation, and downregulation of MHC-I. All of the Nef functions affected by inhibitor treatment are also attenuated by a Nef mutant that is defective for homodimerization, suggesting a common mechanism of action involving altered Nef dynamics or quaternary structure. Structural analysis of Nef in complex with effector proteins and inhibitor analogs is required to shed light on the mechanism of action. Our results also illustrate the value of analog evaluation that combines direct binding assays with preliminary screening against HIV-1 in a cell-based assay. Integrated analysis of data from both approaches identified compounds with potent antiretroviral activity in donor PBMCs that retained the ability to restore cell-surface MHC-I. Future studies will address the efficacy of these compounds in animal models of acute and persistent HIV-1 infection, where Nef expression has been established as a key factor in viral pathogenesis[39–41]. Because of the variability in Nef sequences present in the HIV-1 subtypes responsible for the global AIDS pandemic, it will also be very important to test the active analogs against additional Nef variants. While Nef sequences are indeed diverse, residues critical to the structure of the folded core domain are highly conserved, as are those involved in each of the functions tested in the present study with the inhibitors. In our original report describing the discovery of **B9**, we demonstrated antiretroviral activity against a family of HIV-1 NL4–3 variants carrying Nef sequences representative of all of the major M-group subtypes[24]. These observations suggest that the B9 analogs reported here may also be broadly active.

EXPERIMENTAL SECTION

Sources of materials as well as detailed methods including Nef inhibitor analog synthesis and analytical data are provided in the Supporting Information. Purity of each compound tested in this study was confirmed to be 95% or greater by LC-MS.

Supplementary Material

Refer to Web version on PubMed Central for supplementary material.

ACKNOWLEDGMENTS

The authors thank Drs. Thomas Haimowitz and Hong Ye of the Fox Chase Chemical Diversity Center (FCCDC) for assistance with organic synthesis, and Dr. Mark Brockman of Simon Fraser University for providing the CEM-SS cell system. This work was supported by National Institutes of Health Grants AI057083 and AI126617 to T.E.S. and NIH Small Business Technology Transfer (STTR) grant support to FCCDC in partnership with the University of Pittsburgh (GM112516, T.E.S. Principal Investigator).

REFERENCES

1. Deeks SG; Lewin SR; Havlir DV The end of AIDS: HIV infection as a chronic disease. Lancet 2013, 382 (9903), 1525–1533. [PubMed: 24152939]
2. Sengupta S; Siliciano RF Targeting the Latent Reservoir for HIV-1. Immunity. 2018, 48 (5), 872–895. [PubMed: 29768175]

3. Temesgen Z; Warnke D; Kasten MJ Current status of antiretroviral therapy. Expert. Opin. Pharmacother 2006, 7 (12), 1541–1554. [PubMed: 16872258]

4. Malim MH; Emerman M HIV-1 accessory proteins--ensuring viral survival in a hostile environment. Cell Host Microbe 2008, 3 (6), 388–398. [PubMed: 18541215]

5. Ali A; Wang J; Nathans RS; Cao H; Sharova N; Stevenson M; Rana TM Synthesis and structure-activity relationship studies of HIV-1 virion infectivity factor (Vif) inhibitors that block viral replication. ChemMedChem. 2012, 7 (7), 1217–1229. [PubMed: 22555953]

6. Huang W; Zuo T; Luo X; Jin H; Liu Z; Yang Z; Yu X; Zhang L; Zhang L Indolizine Derivatives as HIV-1 VIF-ElonginC Interaction Inhibitors. Chem. Biol Drug Des 2013, 81 (6), 730–741. [PubMed: 23405965]

7. Arora VK; Fredericksen BL; Garcia JV Nef: agent of cell subversion. Microbes. Infect 2002, 4 (2), 189–199. [PubMed: 11880052]

8. Saksela K Interactions of the HIV/SIV pathogenicity factor Nef with SH3 domain-containing host cell proteins. Curr. HIV. Res 2011, 9 (7), 531–542. [PubMed: 22103837]

9. Joseph AM; Kumar M; Mitra D Nef: “necessary and enforcing factor” in HIV infection. Curr. HIV. Res 2005, 3 (1), 87–94. [PubMed: 15638726]

10. O’Neill E; Kuo LS; Krisko JF; Tomchick DR; Garcia JV; Foster JL Dynamic evolution of the human immunodeficiency virus type 1 pathogenic factor, Nef. J. Virol 2006, 80 (3), 1311–1320. [PubMed: 16415008]

11. Foster JL; Garcia JV HIV-1 Nef: at the crossroads. Retrovirology. 2008, 5, 84. [PubMed: 18808677]

12. Pawlak EN; Dikeakos JD HIV-1 Nef: a master manipulator of the membrane trafficking machinery mediating immune evasion. Biochim. Biophys. Acta 2015, 1850 (4), 733–741. [PubMed: 25585010]

13. Doria M Role of the CD4 down-modulation activity of Nef in HIV-1 infectivity. Curr. HIV. Res 2011, 9 (7), 490–495. [PubMed: 22103832]

14. Rosa A; Chande A; Ziglio S; De S,V; Bertorelli R; Goh SL; McCauley SM; Nowosielska A; Antonarakis SE; Luban J; Santoni FA; Pizzato M HIV-1 Nef promotes infection by excluding SERINC5 from virion incorporation. Nature 2015, 526 (7572), 212–217. [PubMed: 26416734]

15. Usami Y; Wu Y; Gottlinger HG SERINC3 and SERINC5 restrict HIV-1 infectivity and are counteracted by Nef. Nature 2015, 526 (7572), 218–223. [PubMed: 26416733]

16. Bregnard C; Zamborlini A; Leduc M; Chafey P; Camoin L; Saib A; Benichou S; Danos O; Basmaciogullari S Comparative proteomic analysis of HIV-1 particles reveals a role for Ezrin and EHD4 in the Nef-dependent increase of virus infectivity. J. Virol 2013, 87 (7), 3729–3740. [PubMed: 23325686]

17. Fackler OT; Luo W; Geyer M; Alberts AS; Peterlin BM Activation of Vav by Nef induces cytoskeletal rearrangements and downstream effector functions. Mol. Cell 1999, 3 (6), 729–739. [PubMed: 10394361]

18. Tarafdar S; Poe JA; Smithgall TE The Accessory Factor Nef Links HIV-1 to Tec/Btk Kinases in an Src Homology 3 Domain-dependent Manner. J Biol Chem. 2014, 289 (22), 15718–15728. [PubMed: 24722985]

19. Readinger JA; Mueller KL; Venegas AM; Horai R; Schwartzberg PL Tec kinases regulate T-lymphocyte development and function: new insights into the roles of Itk and Rlk/Txk. Immunol. Rev 2009, 228 (1), 93–114. [PubMed: 19290923]

20. Saksela K HIV-1 Nef and host cell protein kinases. Front. Biosci 1997, 2, D606–D618. [PubMed: 9388166]

21. Ren X; Park SY; Bonifacino JS; Hurley JH How HIV-1 Nef hijacks the AP-2 clathrin adaptor to downregulate CD4. Elife. 2014, 3, e01754.

22. Jia X; Singh R; Homann S; Yang H; Guatelli J; Xiong Y Structural basis of evasion of cellular adaptive immunity by HIV-1 Nef. Nat. Struct. Mol. Biol 2012, 19 (7), 701–706. [PubMed: 22705789]

23. Alvarado JJ; Tarafdar S; Yeh JI; Smithgall TE Interaction with the Src homology (SH3-SH2) region of the Src-family kinase Hck structures the HIV-1 Nef dimer for kinase activation and effector recruitment. J Biol Chem. 2014, 289, 28539–28553. [PubMed: 25122770]

24. Emert-Sedlak LA; Narute P; Shu ST; Poe JA; Shi H; Yanamala N; Alvarado JJ; Lazo JS; Yeh JI; Johnston PA; Smithgall TE Effector Kinase Coupling Enables High-Throughput Screens for Direct HIV-1 Nef Antagonists with Antiretroviral Activity. Chem. Biol 2013, 20 (1), 82–91. [PubMed: 23352142]
25. Mujib S; Saiyed A; Fadel S; Bozorgzad A; Aidarus N; Yue FY; Benko E; Kovacs C; Emert-Sedlak L; Smithgall TE; Ostrowski MA Pharmacologic HIV-1 Nef Blockade Enhances the Recognition and Elimination of Latently HIV-1 Infected CD4 T cells by Autologous CD8 T cells. J. Clin. Invest. Insight 2017, 2 (17), e93684.
26. Copeland RA The drug-target residence time model: a 10-year retrospective. Nat. Rev. Drug Discov 2016, 15 (2), 87–95. [PubMed: 26678621]
27. Gervaix A; West D; Leoni LM; Richman DD; Wong-Staal F; Corbeil J A new reporter cell line to monitor HIV infection and drug susceptibility in vitro. Proc. Natl. Acad. Sci. U. S. A 1997, 94 (9), 4653–4658. [PubMed: 9114046]
28. Moroco JA; Alvarado JJ; Staudt RP; Wales TE; Smithgall TE; Engen JR Remodeling of HIV-1 Nef Structure by Src-Family Kinase Binding. J. Mol. Biol 2018, 430 (3), 310–321. [PubMed: 29258818]
29. Trible RP; Narute P; Emert-Sedlak LA; Alvarado JJ; Atkins K; Thomas L; Kodama T; Yanamala N; Korotchenko V; Day BW; Thomas G; Smithgall TE Discovery of a diaminoquinoxaline benzenesulfonamide antagonist of HIV-1 Nef function using a yeast-based phenotypic screen. Retrovirology. 2013, 10, 135. [PubMed: 24229420]
30. Readinger JA; Schiralli GM; Jiang JK; Thomas CJ; August A; Henderson AJ; Schwartzberg PL Selective targeting of ITK blocks multiple steps of HIV replication. Proc. Natl. Acad. Sci. U. S. A 2008, 105 (18), 6684–6689. [PubMed: 18443296]
31. Andreotti AH; Schwartzberg PL; Joseph RE; Berg LJ T-cell signaling regulated by the Tec family kinase, Itk. Cold Spring Harb. Perspect. Biol 2010, 2 (7), a002287.
32. Rekas A; Alattia JR; Nagai T; Miyawaki A; Ikura M Crystal structure of venus, a yellow fluorescent protein with improved maturation and reduced environmental sensitivity. J. Biol. Chem 2002, 277 (52), 50573–50578. [PubMed: 12370172]
33. Lee C-H; Saksela K; Mirza UA; Chait BT; Kuriyan J Crystal structure of the conserved core of HIV-1 Nef complexed with a Src family SH3 domain. Cell 1996, 85, 931–942. [PubMed: 8681387]
34. Poe JA; Vollmer L; Vogt A; Smithgall TE Development and Validation of a High-Content Bimolecular Fluorescence Complementation Assay for Small-Molecule Inhibitors of HIV-1 Nef Dimerization. J Biomol. Screen 2014, 19, 556–565. [PubMed: 24282155]
35. Trible RP; Emert-Sedlak L; Smithgall TE HIV-1 Nef selectively activates SRC family kinases HCK, LYN, and c-SRC through direct SH3 domain interaction. J. Biol. Chem 2006, 281, 27029–27038. [PubMed: 16849330]
36. Emert-Sedlak L; Kodama T; Lerner EC; Dai W; Foster C; Day BW; Lazo JS; Smithgall TE Chemical library screens targeting an HIV-1 accessory factor/host cell kinase complex identify novel antiretroviral compounds. ACS Chem. Biol 2009, 4 (11), 939–947. [PubMed: 19807124]
37. Pereira EA; daSilva LL HIV-1 Nef: taking control of protein trafficking. Traffic. 2016, 17 (9), 976–996. [PubMed: 27161574]
38. Anmole G; Kuang XT; Toyoda M; Martin E; Shahid A; Le AQ; Markle T; Baraki B; Jones RB; Ostrowski MA; Ueno T; Brumme ZL; Brockman MA A robust and scalable TCR-based reporter cell assay to measure HIV-1 Nef-mediated T cell immune evasion. J Immunol. Methods 2015, 426, 104–113. [PubMed: 26319395]
39. Zou W; Denton PW; Watkins RL; Krisko JF; Nochi T; Foster JL; Garcia JV Nef functions in BLT mice to enhance HIV-1 replication and deplete CD4+CD8+ thymocytes. Retrovirology. 2012, 9, 44. [PubMed: 22640559]
40. Watkins RL; Foster JL; Garcia JV In vivo analysis of Nef's role in HIV-1 replication, systemic T cell activation and CD4(+) T cell loss. Retrovirology. 2015, 12, 61. [PubMed: 26169178]
41. Honeycutt JB; Thayer WO; Baker CE; Ribeiro RM; Lada SM; Cao Y; Cleary RA; Hudgens MG; Richman DD; Garcia JV HIV persistence in tissue macrophages of humanized myeloid-only mice during antiretroviral therapy. Nat. Med 2017, 23 (5), 638–643. [PubMed: 28414330]

42. Naidoo L; Mzobe Z; Jin SW; Rajkoomar E; Reddy T; Brockman MA; Brumme ZL; Ndung'u T; Mann JK Nef-mediated inhibition of NFAT following TCR stimulation differs between HIV-1 subtypes. Virology 2019, 531, 192–202. [PubMed: 30927712]

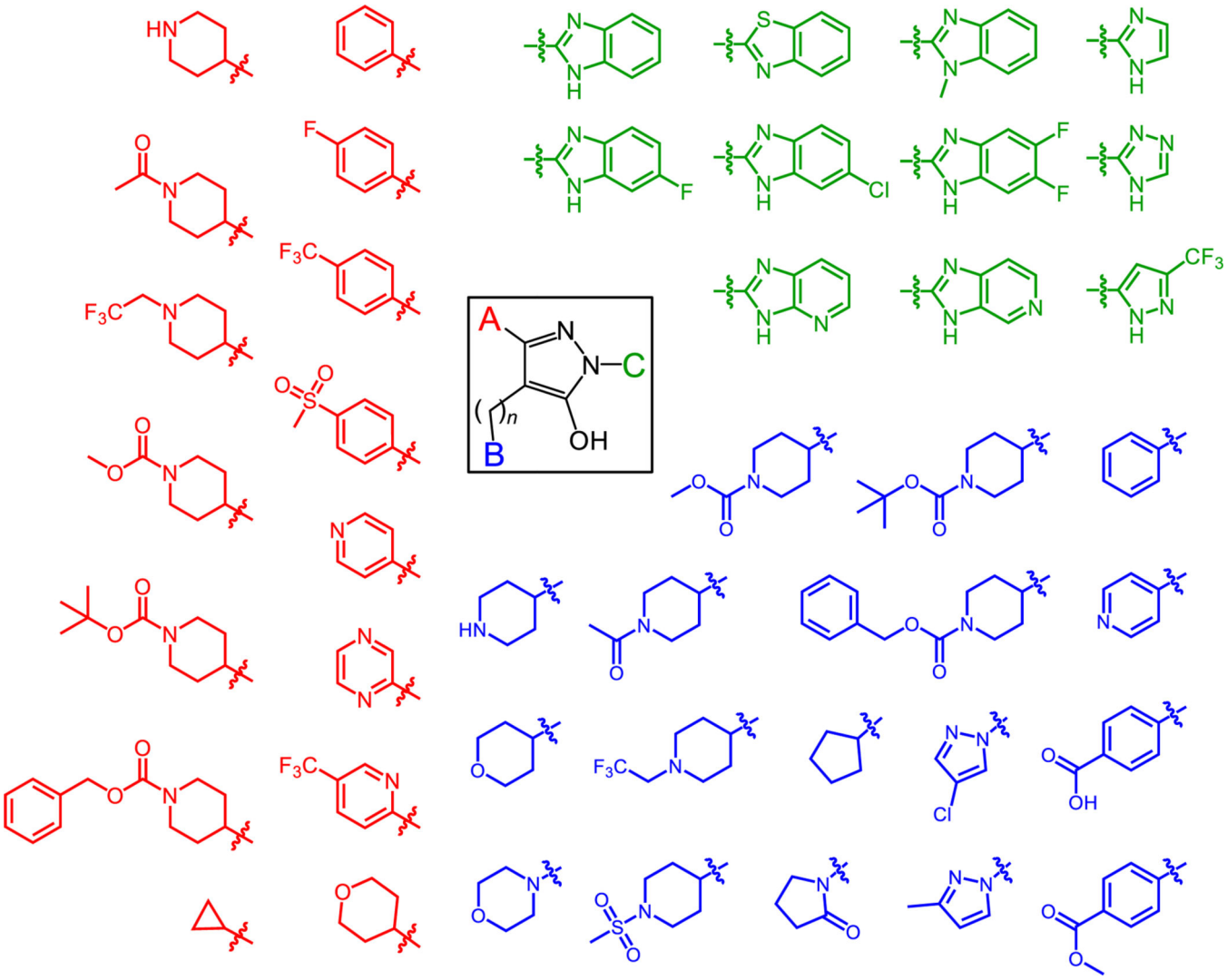

Figure 1. Diversity of hydroxypyrazole HIV-1 Nef inhibitor structures synthesized for this study.

The hydroxypyrazole core found in the HIV-1 Nef inhibitor **B9** is shown at the center, with three functionalities available for medicinal chemistry optimization (A, red; B, blue; and C, green). Representative groups introduced at each position are indicated. The structures of the 170 analogs that interacted with Nef by SPR are shown in the Supporting Information (Table S1). The linker connecting the B group to the pyrazole can be 1 or 2 carbons in length.

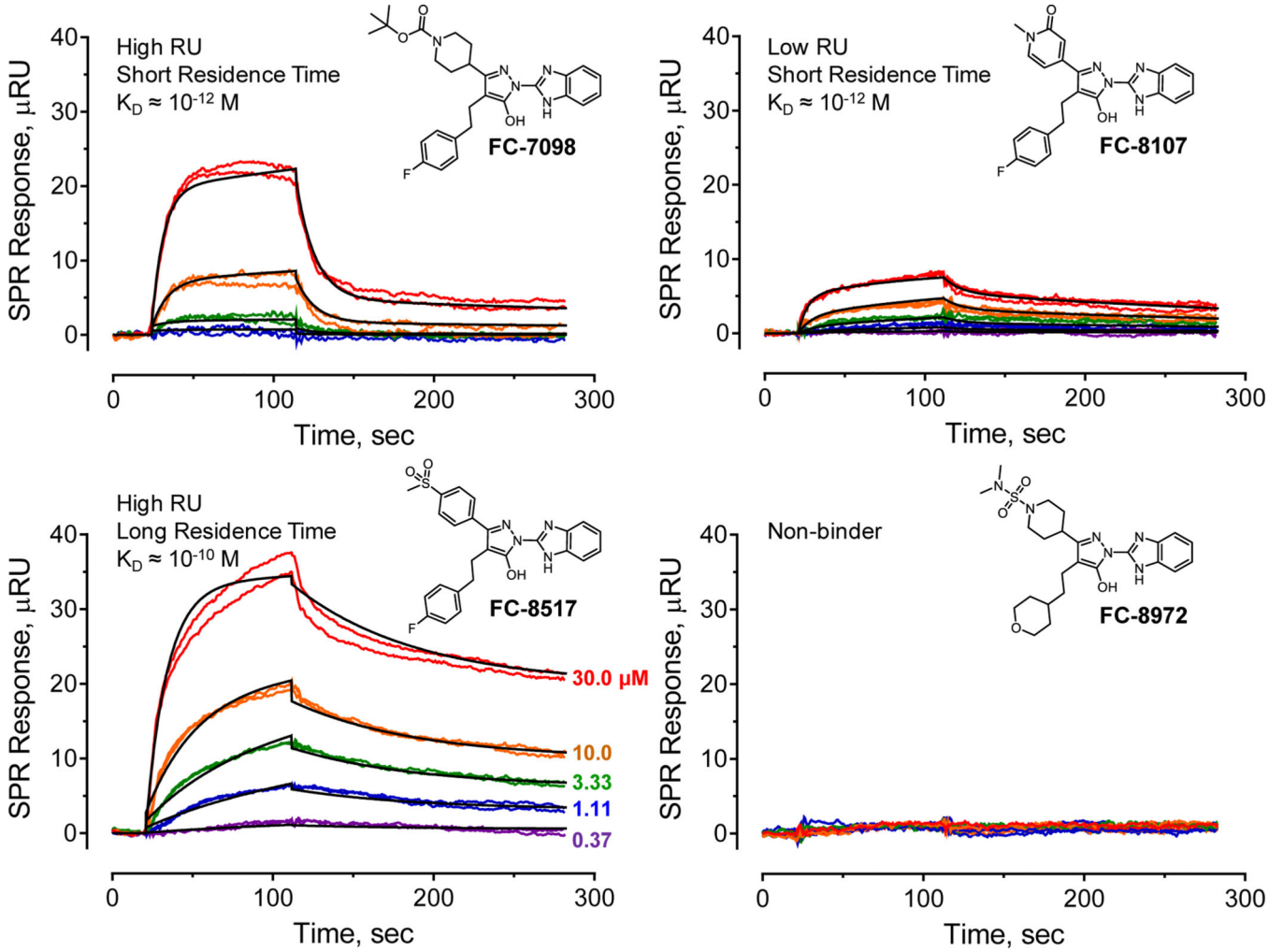

Figure 2. Representative examples of Nef interaction with hydroxypyrazole inhibitor analogs by SPR.

Recombinant HIV-1 Nef protein (strain NL4–3) was expressed in *E. coli* and purified to homogeneity. The Nef protein was covalently immobilized on the surface of a carboxymethyl dextran hydrogel biosensor chip, and each analog was injected over a range of concentrations in duplicate (concentrations shown at lower left) for 90 seconds, followed by a 180 second dissociation phase. The resulting sensorgrams were best fit by either a 1:1 Langmuir binding model or by a two-step induced-fit model, and the K_D values shown were calculated from the resulting kinetic rate constants. Four types of binding behavior were typically observed, and representative examples of each are shown for the indicated analogs. The SPR data for each analog concentration are shown in color, and a single fitted curve is superimposed in black.

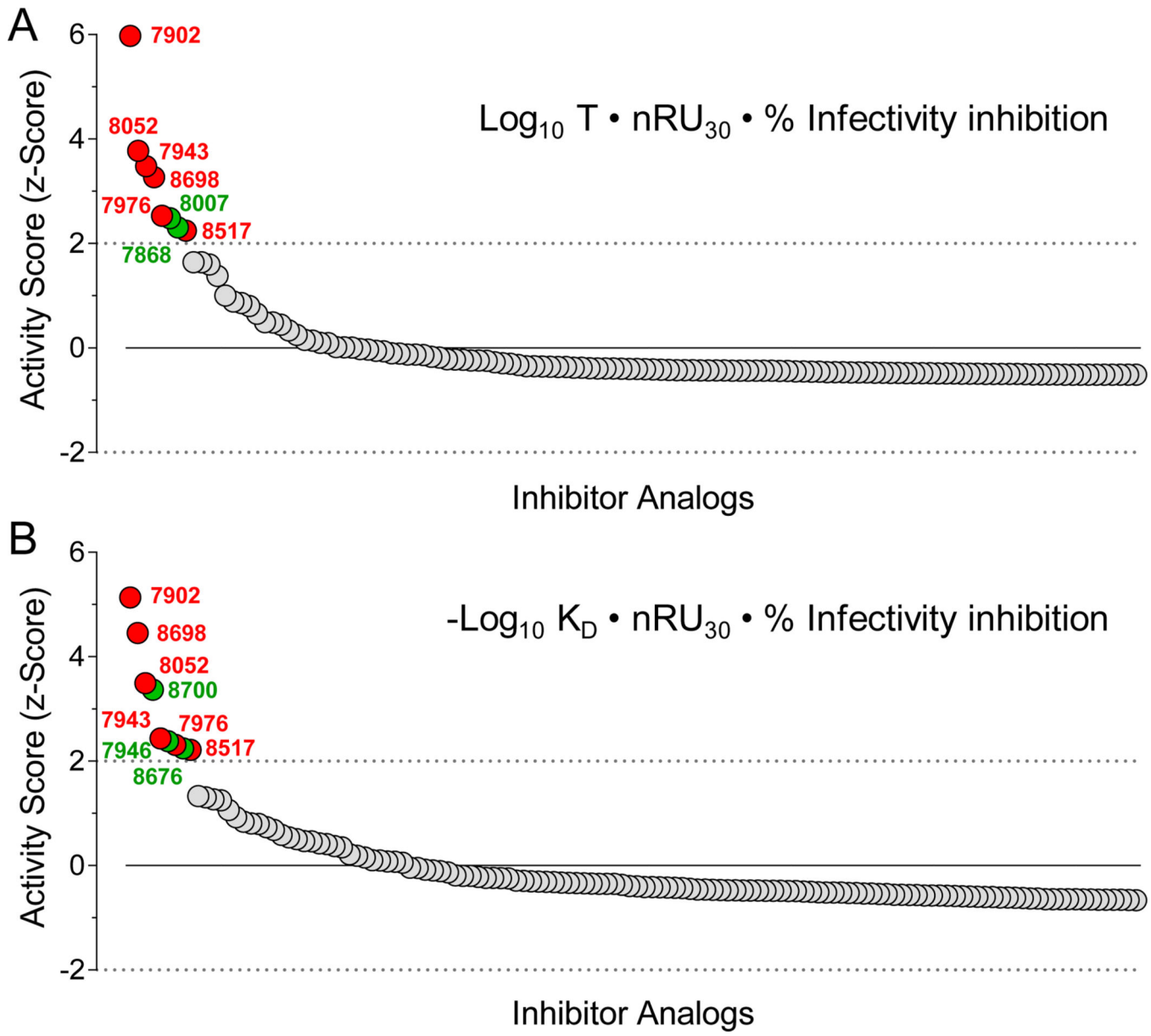

Figure 3. Integration of SPR and infectivity data enables ranking of Nef inhibitor analog activity.

Factors combined to define an 'Activity Score' for each inhibitor analog include analog residence time on Nef during the dissociation phase of SPR analysis ($T = 1/k_{off}$), affinity based on the kinetic K_D from SPR, extent of binding by SPR, and antiretroviral activity (% infectivity inhibition). The extent of binding is based on SPR response units (RU) observed at the highest analog concentration tested (30 μM; RU_{30} value) normalized to the amount of Nef protein immobilized on each chip (RU_{Nef}) such that $nRU_{30} = RU_{30}/RU_{Nef}$. A z-score was then calculated for each compound relative to the mean of all non-zero Activity Scores. In panel A, the Activity Score z-scores were calculated based on the analog residence time, while panel B shows the Activity Score z-score distribution based on K_D as per the respective formulas shown. Compounds with z-scores > 2.0 and common to both analyses

are shown as red data points along with the analog numbers, with unique compounds highlighted in green.

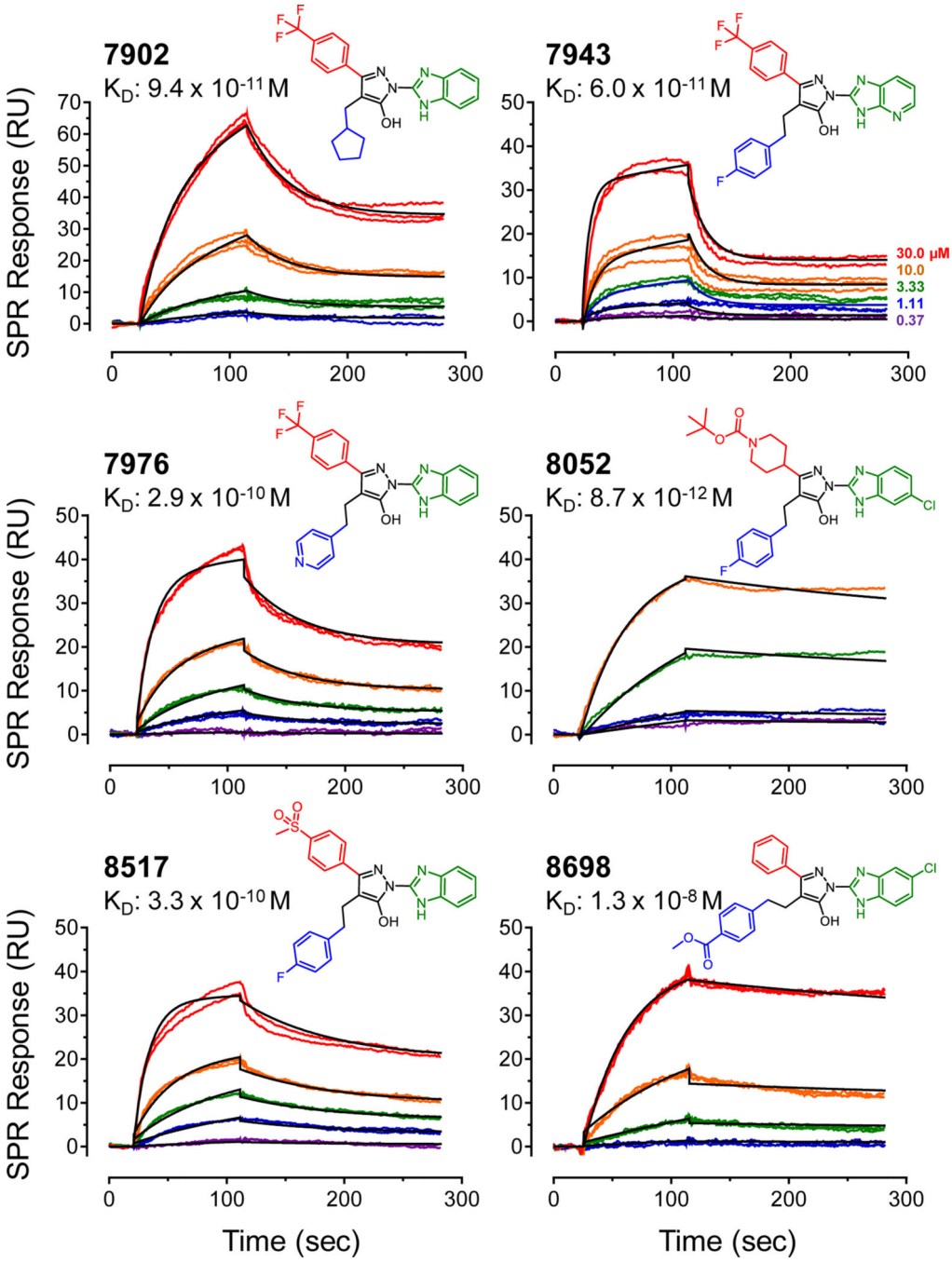

Figure 4. Structures and SPR sensorgrams for top-scoring hydroxypyrazole Nef inhibitor analogs.

Each of the analogs shown was assayed for interaction with HIV-1 $Nef_{NL4–3}$ by SPR as described in the legend to Figure 2. Compounds were tested over the range of concentrations shown, and the resulting sensorgrams were best-fit by a two-step induced-fit model. The SPR data for each analog concentration (top right) are shown in color, and the fitted curves are superimposed in black. The resulting K_D values are shown below each analog number. The A, B and C substituents present in each analogs are shown in red, blue and green, respectively.

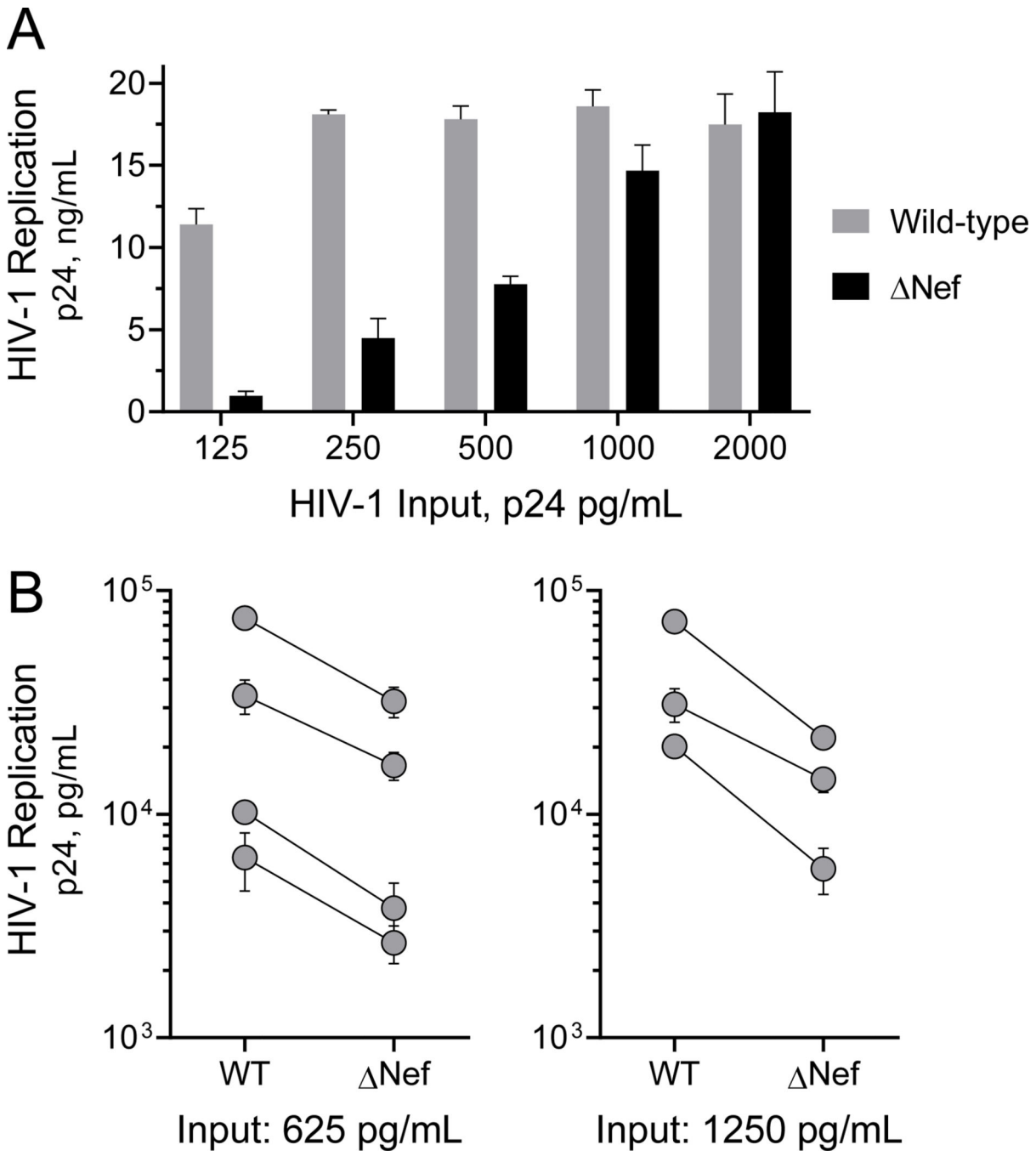

Figure 5. HIV-1 Nef enhances HIV-1 replication in donor PBMCs.

PBMCs were isolated from HIV-negative donor blood and activated with PHA and IL-2. A) PBMCs from a representative donor were infected with wild-type and Nef-defective (ΔNef) HIV-$1_{NL4–3}$ over the range of viral inputs shown, and replication was assessed by HIV-1 p24 Gag using an AlphaLISA assay (Perkin Elmer) after 4 days in culture. B) PBMCs from seven additional donors were infected with wild-type or ΔNef HIV-1 with either 625 or 1,250 p24 equivalents per mL as shown. Replication was assessed by p24 Gag AlphaLISA 4

days later. Each symbol represents the average of three endpoints ± SE for an individual donor, with the wild-type (WT) and ΔNef values connected by a solid line.

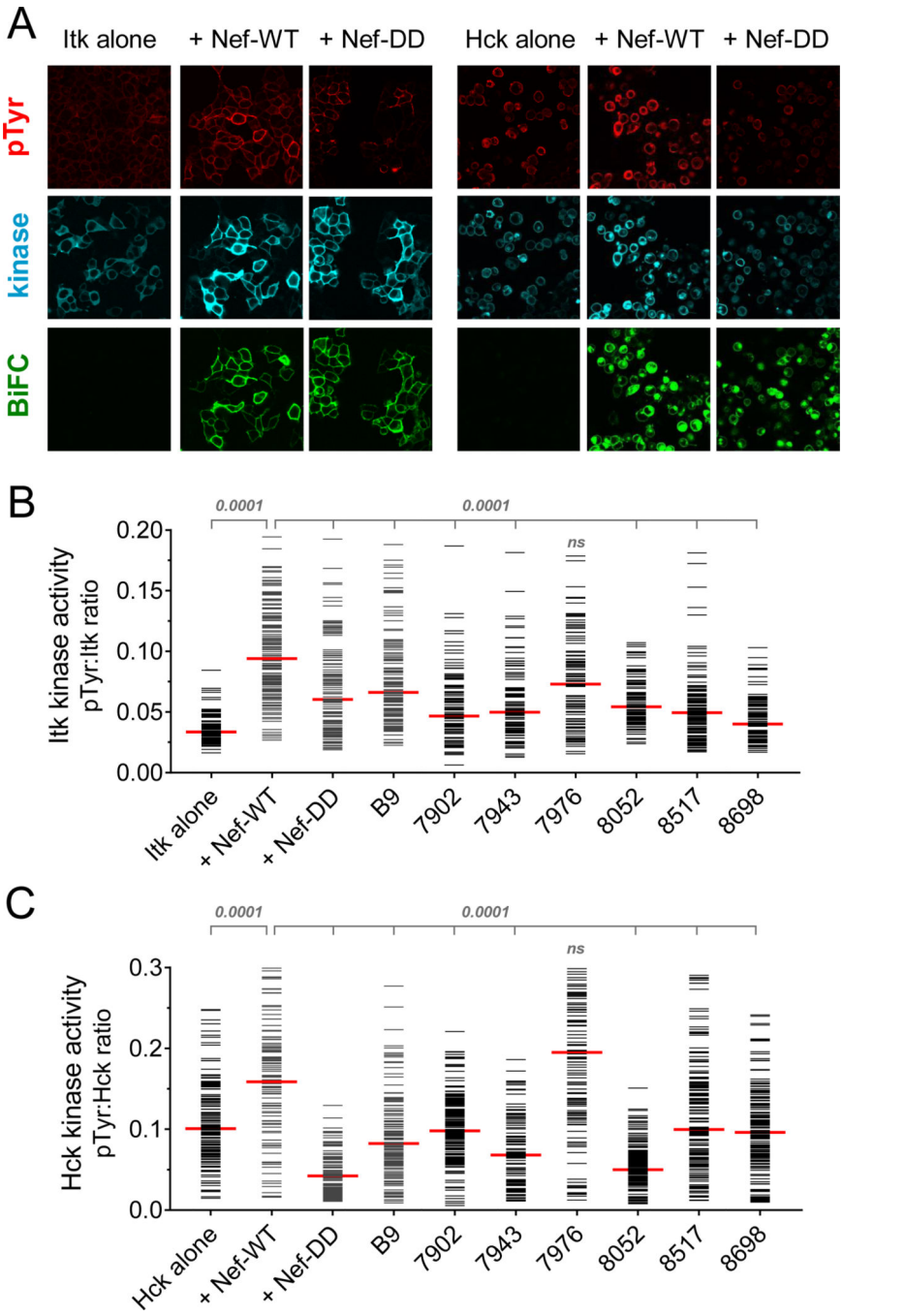

Figure 6. Hydroxypyrazole analogs with antiretroviral activity block Nef-dependent Itk and Hck kinase activation.

Itk or Hck were expressed either alone or together with wild-type Nef (WT) or a homodimerization-defective Nef mutant (DD) as BiFC pairs in 293T cells. Replicate cultures were treated with the Nef inhibitor **B9** or the analogs shown at a final concentration of 1.0 μM. Cells were fixed and immunostained for confocal microscopy with anti-pTyr antibodies as a measure of Itk activity (red) and to the Itk or Hck protein (V5 epitope; blue) to verify expression. For Hck, kinase activity was assessed by immunostaining with a

phosphospecific antibody to the activation loop phosphotyrosine, pY416. Nef interaction with Itk or Hck was recorded as fluorescence of the complemented Venus variant of YFP (BiFC; green). A) Representative confocal images of control cultures. B,C) Single-cell image analysis. Mean fluorescence intensities for the pTyr and Itk signals (B) or the pY416 and Hck signals (C) were determined for a minimum of 100 cells from each condition using ImageJ. Fluorescence intensity ratios (pTyr:kinase protein expression) were calculated and are presented as horizontal bars for each cell; the median value is represented by the large red bar. Pairwise Student's t-tests were performed on ratios obtained with Itk alone vs. Itk + Nef-WT ($p < 0.0001$) and on Itk + Nef-WT vs. Itk + Nef-DD as well as each inhibitor group ($p < 0.0001$ in all cases except cells treated with **FC-7976**.

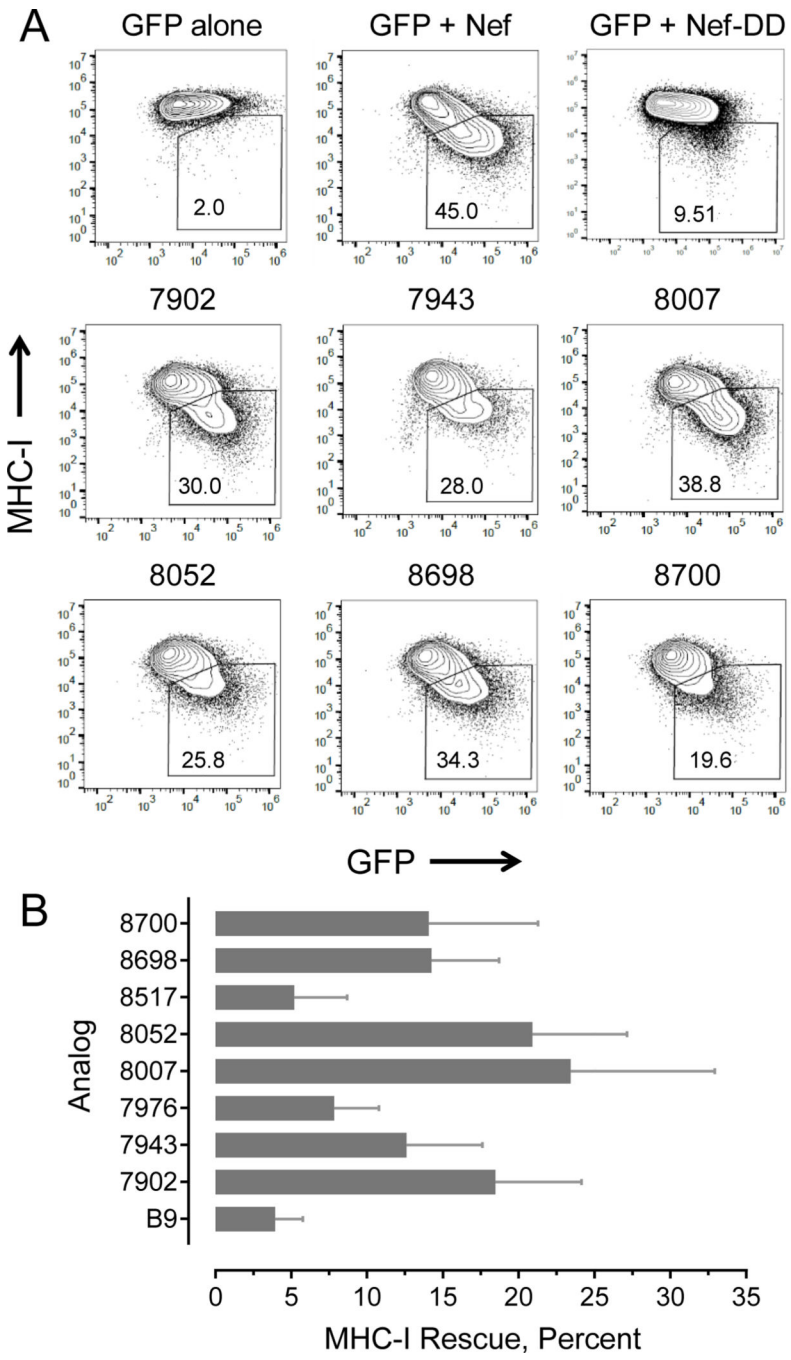

Figure 7. Hydroxypyrazole HIV-1 Nef inhibitors rescue cell-surface MHC-I in Nef-transfected cells.

The CEM-SS T cell line, which is engineered to over-express an HLA-A2 allele, was transfected with an expression plasmid for HIV-1 Nef plus GFP as a gating marker. Cells transfected with GFP and Nef were incubated in the presence of **B9** and the inhibitor analogs shown. After 48 hours, cells were fixed and stained for cell-surface HLA-A2 and analyzed by flow cytometry. A) Representative flow cytometry plots showing the percentage of GFP^{+}/ $MHC\text{-}I^{-}$ cells in the presence and absence of select compounds (*box*). The dimerization-defective Nef mutant Nef-DD is included as a negative control. B) Cell-surface MHC-I

rescue by Nef inhibitor analogs based on median fluorescence intensity of MHC-I^+ cells and the following formula: $[(Nef^+MHC^+/Nef^-MHC\text{-}I^+)_{drug} - (Nef^+MHC^+/Nef^-MHC\text{-}I^+)_{no\ drug}]$ x 100, where Nef^+ cells are defined by GFP expression (analysis as per Naidoo, *et al.*[42]). Bars represent mean values ± S.E. with 3 to 5 biological replicates in each case.

Table 1.

Inhibition of HIV-1 replication by hydroxypyrazole Nef inhibitor analogs in PBMCs.

Donor PBMCs were infected with HIV-1 in the presence of inhibitor concentrations ranging from 1 to 1,000 nM or the DMSO carrier solvent as a negative control (0.1% DMSO final). Replication was assessed by p24 Gag AlphaLISA (Perkin Elmer) five days later. Each donor was also infected with Nef-defective HIV-1 to establish the baseline for Nef-dependent enhancement of replication in each culture. Cytotoxicity was assessed in uninfected PBMCs over the same incubation period using the CellTiter-Blue assay (Promega). Data were fit by non-linear regression analysis (GraphPad Prism v.7.04) to determine the IC_{50} and CC_{50} values shown. Results with the original hit compound, **B9**, are included for comparison. n/d, not determined.

Analog	HIV-1 Replication IC_{50}, nM	Cell Viability CC_{50}, nM	Therapeutic Index CC_{50}/IC_{50}
FC-7902	5.0	1,952	390
FC-7943	2.5	1,806	1,015
FC-7976	1.8	1,563	878
FC-8052	0.7	760	1,169
FC-8517	9.5	6,442	678
FC-8698	31.9	1,153	36
B9	72.2	> 1,000	n/d